U. S. NAVY

MARINE ENGINEERING LABORATORY

Annapolis, Md.

Dedicated To PROGRESS IN MARINE ENGINEERING

Charge-Current Control Circuit for
Nickel-Cadmium Cells with Control Electrodes

Assignment 61 501
MEL Research and Development Report 25/65
April 1965

By
P. P. M. Liwski

P. P. M. Liwski (signature)

P. P. M. LIWSKI

Approved by:

R. J. Wylde (signature)

R. J. WYLDE
Electrical Systems Division

Distribution List

BUSHIPS, Code 210L (2)
DDC (20)
NASA Battery Test Facility
    Naval Ammunition Depot
    Crane, Indiana (3)
Addressee (10)

DDC Availability Notice - Qualified requesters may obtain copies of this
report from DDC.

2 4894

ABSTRACT

A circuit to control charge current entering
nickel-cadmium cells with control electrodes
("three-terminal" cells) has been developed by MEL
for use in systems requiring minimum space and
weight with optimum control. The potential on the
third (control) electrode of a cell becomes input
to determine time and manner of charge-current
change. Presently a laboratory instrument, this
circuit is later to be adapted to satellite appli-
cations.

author

ADMINISTRATIVE INFORMATION

TABLE OF CONTENTS

CHARGE-CURRENT CONTROL CIRCUIT FOR
NICKEL-CADMIUM CELLS WITH CONTROL ELECTRODES

1.0 INTRODUCTION

1.1 Background. The charge-current control circuit for nickel-cadmium
cells with control electrodes ("three-terminal" cells) was designed to
meet the requirements of this latest development in secondary cells. In
the past automatic charging of nickel-cadmium cells to a nominal 100
percent of their rated capacity, then holding them in this condition with
a trickle charge until needed, was very difficult. Their easily measured
terminal voltage could not be used as an indicating signal for control
circuitry, since it is relatively flat throughout the normal range of
cell-charge conditions. Extraordinarily complex circuitry has been used
to perform this task, but it still did not provide good charge-current
control. Undercharging the cells resulted in reduced capability, and
overcharging resulted in danger of explosion due to gas generation in
the cells. The possibility of inconsistent control is a decided dis-
advantage in satellite applications where all systems must be optimized
because of the weight and space problem.

1.2 Problem. Recently, nickel-cadmium cells have been developed with a
third electrode whose potential (with respect to the negative cell termi-
nal) is a direct function of the number of oxygen molecules in the cell.
When a nickel-cadmium cell is being charged, it generates oxygen very
slowly until it nears its rated maximum charge condition, when suddenly
the amount of oxygen generated internally increases rapidly. The in-
creasing numbers of oxygen molecules impinging on the third electrode
produce a fast rising potential there.

The charge-current control circuit described here utilizes this
potential from each cell in a group or battery to determine when and
how much charge current is required to obtain optimum cell-charge con-
dition. This circuit is designed to monitor the third-therminal po-
tential of each cell in a group of five while they are being charged.
As the third-terminal potential rises above a set value in any one of
the cells in the group, the circuit begins reducing the charge current
to the series group of cells, so that when the third-terminal potential
of any cell reaches a predetermined maximum, the charge current will
have been reduced to a preset trickle charge or to zero.

A detailed description of the operation of this control circuit is
included in Appendix A; a block diagram of subcircuit functions is shown
in Figure 1 and a complete circuit diagram in Figure 1-A. In its present
form it is for laboratory use only, and with additional detectors it will
accommodate virtually any number of cells. In the future it will be
temperature compensated and otherwise adapted to satellite applications
where wide temperature variations are encountered.

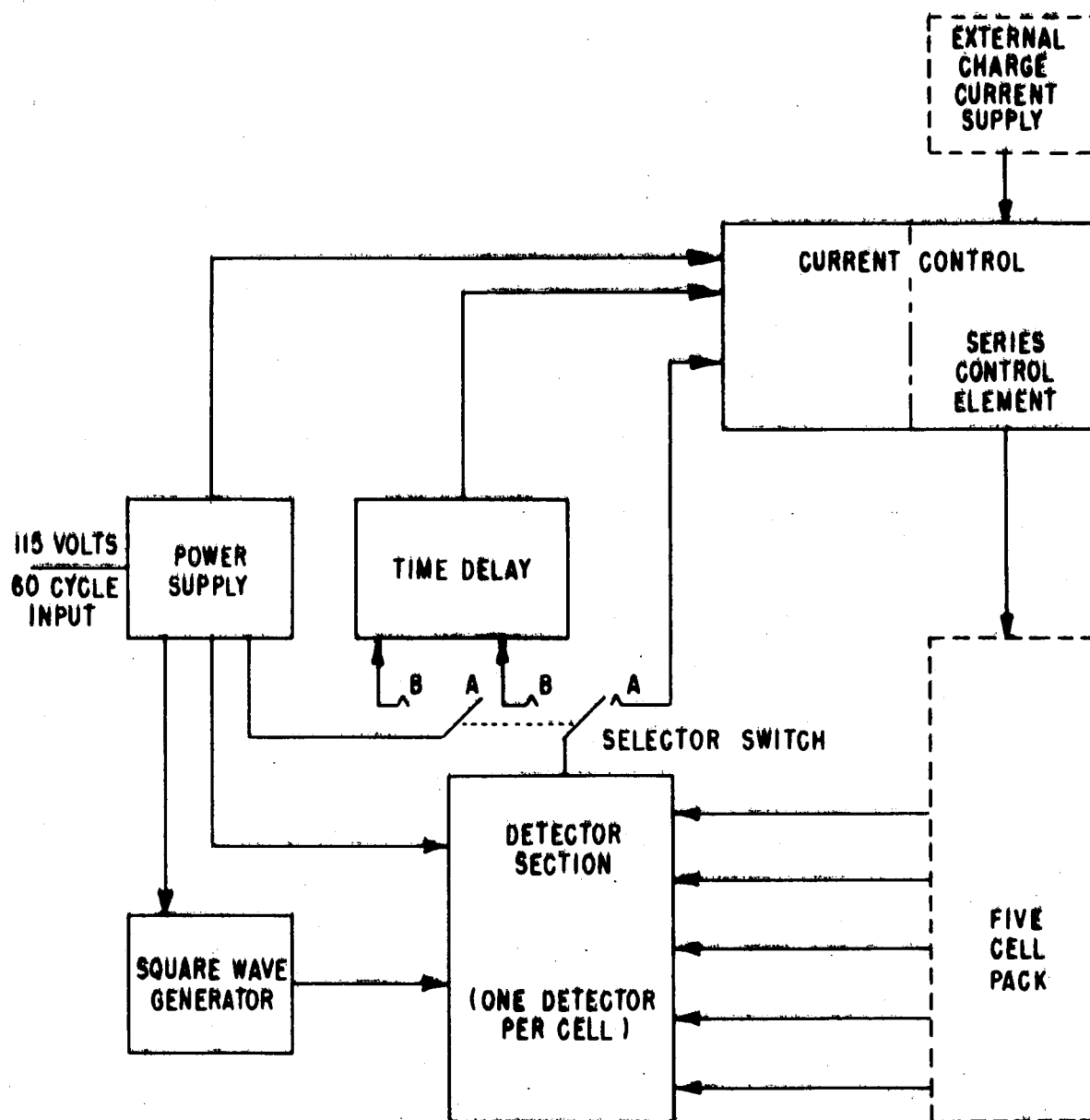USN
MARINE ENGINEERING LABORATORY

Figure 1

Subcircuit Functions

2.0 FUNCTIONAL CIRCUIT DESCRIPTION

The control circuit shown in block diagram form, Figure 1, was designed for use with the two forms of three-terminal cells presently manufactured. The characteristics of the third-terminal potential of these two types of cells are not the same. For circuit-design purposes, the chief difference is that the third-terminal potential of the Type B cell does not begin increasing at the same cell-charged state, and does not increase at the same rate, as that of the Type A cells. This means that the circuit must have two modes of operation, one for each type of cell. A selector switch provides the choice of these two modes. In either mode of operation, both types of cells, after the charge current has been reduced to trickle-charge level, should have been charged to approximately 110 percent of their capacity.

2.1 Subcircuits. The circuit consists of five subcircuits or sections (see Figure 1): a detector section containing a detector for each cell; a square wave generator; a current control section; a time delay section; and a power supply. The basic concept of the operation of the detectors and the versatility of their operating conditions are described in Appendix B.

● Each detector samples the third-terminal potential of its cell 500 times a second and translates this information to a d-c* level.

● The square wave generator provides the sampling signal utilized by the detector section.

● The current-control section uses the d-c level from the detectors to decrease the battery charging current from full charge to a trickle charge, as a cell's third-terminal potential increases. This is accomplished by a series control element. The charge current being controlled is derived from an external supply.

● The time delay section, when used, causes the initial decrease in charging current to be delayed by 5 minutes after a cell's third-terminal potential reaches the level which would normally cause the charge current to begin decreasing. The highest third-terminal potential in the group governs the charging rate of the group.

● The power supply converts 115-volt, 60-cycle line voltage to a d-c bias voltage for use by the other circuit sections.

---

*Abbreviations used in this text are from the GPO Style Manual, 1959, unless otherwise noted.

2.2 The A Mode. When used with the cells from Company A (selector switch in Position A) the circuit admits a full-charge current into the five cells when they are in a discharged state. As any one cell nears its fully charged condition, its third-terminal potential begins to increase from zero. When this potential reaches approximately 125 millivolts (mv), the charge-control section of the circuit begins to decrease the charging current into the cells. As any cell's third-terminal potential increases above 125 mv, the charging current decreases linearly; the current is reduced to a trickle charge when the third-terminal potential of any cell has reached 250 mv. The circuit will remain in this trickle-charge condition as long as a third-terminal potential remains above 250 mv unless the cells are manually disconnected. If all third-terminal potentials fall below 250 mv, the charge current will increase linearly and again be controlled by the highest third-terminal potential.

2.3 The B Mode. With the selector switch in the B position, the circuit will allow a full-charge current into the five discharged cells. However, in this mode, when the third-terminal potential of any cell increases to 125 mv, a 5-minute time delay is initiated. For the next 5 minutes, a full-charge current will continue into the cells, regardless of the condition of their third-terminal potentials. At the end of 5 minutes, control of the charging current will be returned to the cell with the highest third-terminal potential. If this potential is still 125 mv, the full-charge current will continue; if it is between 125 and 250 mv, the charging current will decrease to a value proportional to it; if it is above 250 mv, the charging current will immediately reduce to its trickle-charge level. That is, at the end of the 5-minute time delay, the operation of the circuit in the B mode is identical to the A mode with respect to the third-terminal potentials.

3.0 CONCLUSION

The project to develop the charge-current control circuit for nickel-cadmium cells with control electrodes (three-terminal cells) as a laboratory instrument has been concluded and two prototypes delivered to NASA - Goddard Space Flight Center, Code 636.2. Operating tests have shown that the circuit performs reliably in both modes as intended.

4.0 FUTURE DEVELOPMENT

The circuit described in this report controls the cell-charge current with a series element. In the future a shunt form of current control will be developed for use with detector and amplifier sections similar to those described here. Both forms of this circuit will eventually be temperature compensated, if needed, for operation in the range of -10 to +50 C, and will be modified to derive their bias voltages from the cells under control rather than from a separate power supply. With these changes, the charge-current control circuit will be suitable for satellite applications. The specific application will determine whether a series or shunt control will be required.

Appendix A

Circuit Description of Charge-Current Control Circuit

This appendix refers to Figure A-1 and describes the stage-by-stage operation and adjustments in the main portions of the charge-current control circuit for three-terminal nickel-cadmium cells.

The power supply consists of a standard bridge rectifier, filter, and series voltage regulator. It contains Q_{10} and Q_{11}, D_9 through D_{15}, R_{23} through R_{29}, C_8, L_1, and T_3. It converts 115 volts $\pm$ 10 percent, 60-cycle ac to 10 volts dc $\pm$ 1 percent regulated for a load variation of 100 percent.

The drive flip-flop is a standard type. It consists of Q_5 and Q_6, D_7, R_{10} through R_{13}, C_3, and C_4. It provides a 500-cycle, 4-volt positive square wave to the detectors as a sampling signal.

Each detector consists of Q_4, D_4 through D_6, R_6, R_8, C_2, and T_1. Resistor R_9 is a 47-ohm leakage resistor from the third terminal to the negative terminal of each cell as specified by NASA. If a cell is in a discharged condition, its third-terminal potential is virtually zero; thus, no dc flows through D_6, R_8, and the d-c side of T_1. For the square wave sampling signal in the a-c side of T_1, this path appears as a high impedance. Therefore, the energy of the square wave is stored in C_2, since the path through D_5 and C_2 is a lower impedance. This allows C_2 to maintain a d-c voltage level sufficient to bias Q_4 on in a near saturation state. As the nickel-cadmium cell charges up, its third-terminal potential increases, thus allowing a low d-c current to flow through D_6, R_8, and the d-c side of T_1. As this current increases (with an increasing third-terminal potential), the dynamic impedance of Diode D_6 decreases, thus lowering its reflected impedance as seen by the square wave. As this impedance decreases, more energy is dissipated through T_1 and less is stored in C_2. This will lower the d-c voltage maintained by C_2 and will cause Q_4 to travel through its active region toward cutoff. When Q_4 is near saturation, its collector voltage is held at less than 1 volt, but as it moves through the active region toward cutoff, its collector voltage increases from less than 1 volt toward a maximum of 10 volts (the bias supply). With Diodes D_4 of the five detectors connected at their cathodes, they act as an OR circuit, meaning that the highest anode voltage is the voltage which appears at the cathode connection of the diodes. Therefore, this is the d-c output level of the detector stage.

The current control stage simply inverts a changing d-c voltage level and converts this to a changing d-c current output from an external current supply. This section consists of Q_1 through Q_3, Q_{12}, D_1 through D_3, R_1 through R_5, C_1, SCR_1, S_1, and S_2. With Selector Switch S_1 in the A position, the time delay section is deactivated. A rising detector output voltage (caused by a third-terminal potential rising above 125 mv) will bias the darlington pair Q_{12}, Q_3 on from cutoff toward saturation, thus lowering the collector voltage of Q_{12}, Q_3. As the collector voltage of the darlington pair decreases, the base current of Q_2 is decreased, thus reducing its collector current. A decreasing collector current in Q_2 is the same as a decreasing base current in Q_1. If the base current

of Q_1 is reduced, its collector current is reduced proportionately, thus decreasing the charging current from the external supply into the five nickel-cadmium cells. This will be reduced to trickle-charge level when any third-terminal potential reaches 250 mv.

The time delay section is simply a unijunction-transistor timing circuit adjusted to yield an output pulse 5 minutes after being activated. It consists of Q_7 through Q_9, D_8, R_{14} through R_{21}, R_{30}, C_5 through C_7, C_9, T_2, SCR_2, and SCR_3. With Selector Switch S_1 in the B position, the 10-volt supply is connected to the time-delay circuit, but it is not activated until SCR_2 has been gated "on." Also with S_1 in this position, the emitter of Q_3 will not be connected to ground until SCR_1 has been gated "on." When any third-terminal potential reaches 125 mv, the detector output voltage is at a level sufficient to gate on SCR_2, through the field effect transistor Q_9, thus activating the time-delay circuit. So far in this B mode, Q_3 has been unable to control the remaining portion of the current control section, since its emitter is floating. Therefore, the standing bias condition on Q_2 maintains the charging current at full charge. Five minutes after the activation of the time delay circuit, its output pulse through T_2 will gate on SCR_1, thus allowing the detector output, through Q_{12}, Q_3, to control the value of charging current into the five cells. The same pulse which gated on SCR_1 aslo gated on SCR_3, enabling the energy stored in C_9 to turn off SCR_2 and deactivate the time-delay circuit. Now the value of the charging current will depend on the detector output, and its control will be the same as that described above for the A mode.

There are a number of adjustments possible in both the detector and the current control sections. The value of the third-terminal potential at which the charging current begins to decrease (or at which the time-delay circuit is activated in the case of B mode) can be varied by adjusting R_7. Increasing R_7 will allow the third-terminal potential to rise to a value greater than 125 mv before the charging current begins to decrease. Decreasing R_7 will have just the opposite effect. As this adjustment is made, the value of the third-terminal potential at which the charging current reaches trickle-charge level is varied also, with the difference between the two potentials remaining essentially the same. The variable resistor, R_5, is included as a calibration adjustment. It is generally set when the circuit is first used to account for any difference in the gain of Q_3 from its design value. It is set in conjunction with the initial R_7 adjustments and afterwards only if Q_3 is ever replaced. Its value will be in the neighborhood of 50 kilohms. The trickle-charge value can be varied from less than 1 to greater than 2 amperes by adjusting R_1. By increasing R_1, the value of the trickle charge will be decreased and vice versa. It is possible to achieve a trickle charge of zero by minor circuit modifications. Adjustments to R_1 are made only when S_2 is depressed. Switch S_2 is a normally closed pushbutton switch. Depressing S_2 allows the trickle charge current to be adjusted without any effects from the rest of the control circuitry. The value of the full-charging current can be varied from 5 to 15 amperes by adjusting R_2. Increasing R_2 will decrease the full-charge current value, while decreasing R_2 will increase the full-charge current value. When the full-charge

current is adjusted with R_2, the current limit on the external current supply should also be set for this value. When R_2 is being adjusted, it is preferable to keep Q_1 in saturation. If R_2 is adjusted for the desired full-charge current, and as a result the collector to emitter voltage of Q_1 becomes greater than 0.4 to 0.6 volt, then the output voltage of the external current supply should be reduced to return to this condition. This is done in order to minimize the power dissipation in Q_1.

The power consumed by the full control circuit from the 10-volt bias source is 250 milliwatts, being maximum at a setting of 2-ampere trickle charge for a corresponding full charge of 15 amperes.
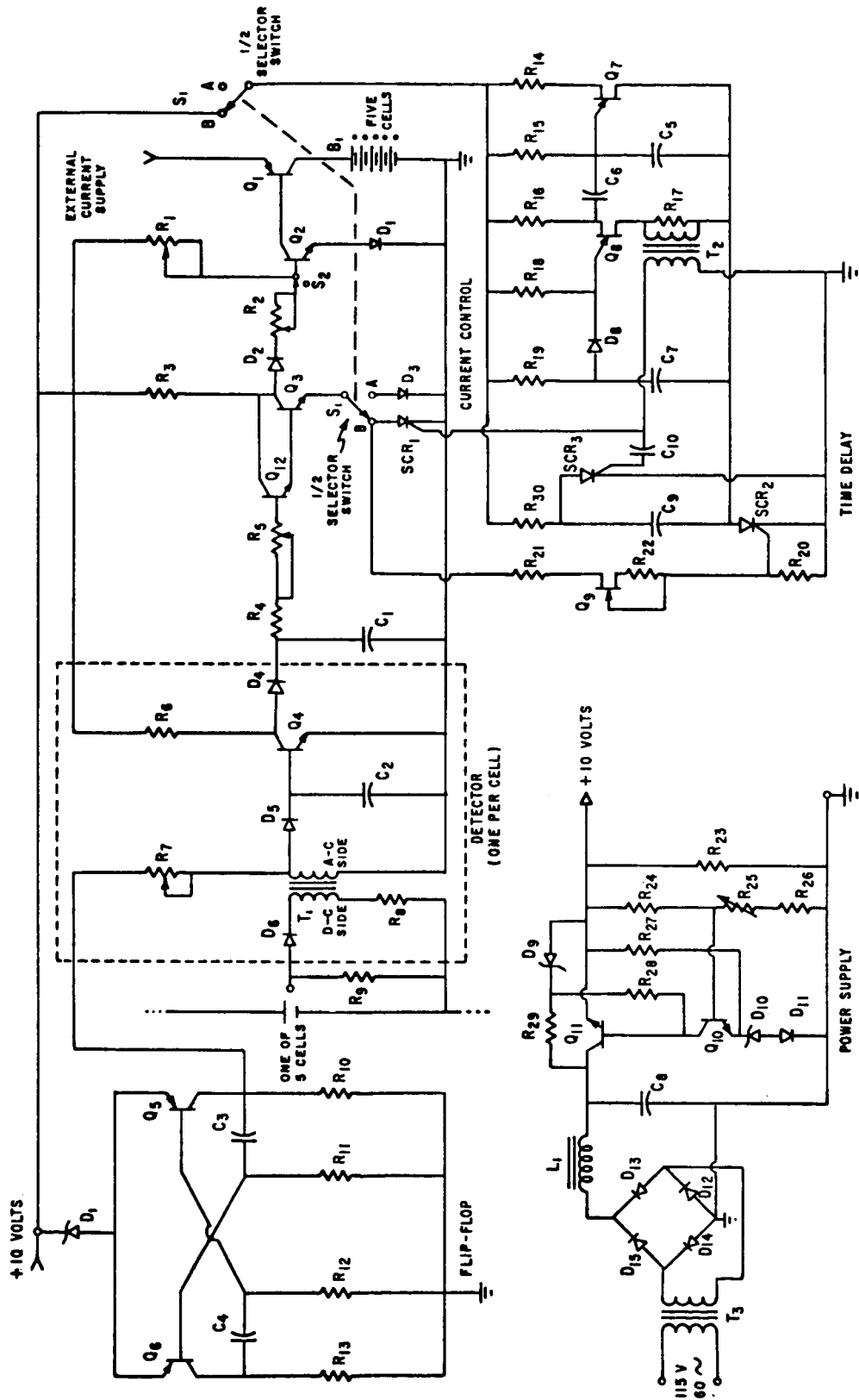
USN MARINE ENGINEERING LABORATORY

Figure 1-A – Charge Current Control Circuit

Parts List for Charge Current Control Circuit

R_1 - 100K Potentiometer
R_2 - 5K Potentiometer
R_3 - 549 ᴧ
R_4 - 1.7 Meg
R_5 - 2 or 5 Meg Potentiometer
R_6 - 10 K
R_7 - 20 K Potentiometer
R_8 - 470 ᴧ
R_9 - 47 ᴧ Specified by NASA
R_{10} - 10 K
R_{11} - 47 K   All resistors
R_{12} - 47 K   1/4 watt
R_{13} - 10 K
R_{14} - 51 ᴧ
R_{15} - 100 K

R_{16} - 51 ᴧ
R_{17} - 100 ᴧ
R_{18} - 5 Meg
R_{19} - 30 Meg
R_{20} - 4.7 K
R_{21} - 19.6 K
R_{22} - 1 K
R_{23} - 220 ᴧ
R_{24} - 620 ᴧ
R_{25} - 1 K Potentiometer
R_{26} - 1 K
R_{27} - 2 K
R_{28} - 3.9 K
R_{29} - 510 ᴧ
R_{30} - 100 K

C_1 - 1 μF
C_2 - 10 μF   All capacitors
C_3 - .033 μF   10 WVDC or
C_4 - .033 μF   more
C_5 - .033 μF
C_6 - .1 μF
C_7 - 10 μF
C_8 - 7000 μF - Sprague Electric
C_9 - 10 μF   36D1070T
C_{10} - .005 μF

D_1 - IN4005
D_2 - JAN IN457
D_3 - IN4005
D_4 - JAN IN457
D_5 - JAN IN457
D_6 - IN191
D_7 - IN752A (ZENER)
D_8 - JAN IN457
D_9 - IN752A (ZENER)
D_{10} - IN752A (Zener)
D_{11} - IN457
D_{12} - IN4005
D_{13} - IN4005
D_{14} - IN4005
D_{15} - IN4005

L_1 - 2 n Choke
       Chicago Standard C-2325
T_1 - 1 : 1 Transformer (Toroid)
       Sprague Electric R1111
T_2 - Interstage Transformer
       U.T.C.   DOT-36
T_3 - Filament Transformer
       Knight 6-K-48 HF
Q_1 - 2N2152 (Wakefield Heat Sink NC-421 B)
Q_2 - 2N1720 (Wakefield Heat Sink NC-302 M)
Q_3 - 2N1613
Q_4 - 2N338
Q_5 - 2N1303
Q_6 - 2N1303
Q_7 - 2N491 (UJT)
Q_8 - 2N494C (UJT)
Q_9 - FE - 202 Amelco Semiconductor
Q_{10} - 2N335
Q_{11} - 2N1613 (Wakefield Heat Sink NF-213)
Q_{12} - 2N338

SCR_1 - 2N1871 or 2N2324
SCR_2 - 2N2324
SCR_3 - 2N2324

S_1 - Dp DT Switch
S_2 - Spring Loaded Push Button
       Switch - normally closed

Figure 1-A (Cont)

Appendix B

Theory of Diode Detector Operation

The circuit diagram of a detector from the charge-current control circuit for nickel-cadmium cells with control electrodes (three-terminal cells) is shown in Figure 1-B. The basic concept which governs the operation of this detector is shown in the equivalent circuit of the input portion of this detector in Figure 2-B. The variable impedance, R_R, in Figure 2-B is the effective impedance of Diode D_6 and Resistor R_8 reflected to the a-c side of the 1 to 1 transformer, T_1. D_6 and R_8 are connected to the d-c side of T_1. The characteristic curve of the D_6, R_8 combination is shown in Figure 3-B. The slope of this curve is equal to the inverse of the impedance of this D_6, R_8 combination. It can be seen from Figure 3-B that, as the voltage across D_6, R_8 increases, the current through them increases and their effective impedance decreases. Therefore, as the potential on the control electrode (third terminal) increases, the effective impedance of D_6, R_8 decreases. The impedance of the d-c side of T_1 remains constant and is small compared to the impedance of D_6, R_8, and is therefore ignored. Now it can be seen from Figures 1-B and 2-B that a rising third-terminal potential, causing a reduction in the reflected impedance, R_R, will decrease the power from the square wave generator available to the amplifying portion of the detector, through D_5 and C_2, by dissipating it in R_R. The square wave generator and Resistor R_7 supply a relatively constant current to the parallel combination of R_R and R_A (the effective impedance of the input to the amplifying portion of the detector) and L, the a-c winding of Transformer T_1. Therefore, as R_R decreases, it will decrease the impedance of this parallel combination, and a smaller voltage drop will appear on the base of Q_4.

Mathematically, this concept is expressed by:

$$R_R = R_8 + R_D$$

$$R_D = \frac{V_D}{I_D}$$

$$I_D = I_R \ (e^{\frac{qV_D}{kT}} - 1) \quad \text{the diode equation}$$

$$R_R = R_8 + \frac{V_D}{I_R(e^{\frac{qV_D}{kT}} - 1)}$$

$$V_D + V_{R_8} = V$$

where

R_D = effective impedance of Diode D_6

V_D = voltage across D_6

I_D = current through D_6

I_R = saturated value of reverse current through D_6

q = electron charge

k = Boltzmann's constant

T = absolute temperature, K

V_{R_8} = voltage across R_p

V = third-terminal potential

It is easily seen that R_R will decrease as $\dot{V}$ increases, since e $q V_D/kT$ increases at a faster rate than V_D alone as V increases. It is understood that R_R and the combined impedance of D_6 and R_8 are identical, since an impedance can be "reflected" from one side of a transformer to the other with a miltiplying factor equal to the transformer turns ratio (in this case, 1 : 1). This proves the inverse dependence of the reflected imped-ance, R_R, on the control electrode (third-terminal) potential of the cell to which this detector is connected.

Also (from Figure 2-B):

$$I_{R_A} = \frac{V_{R_A}}{R_A}$$

$$V_{R_A} = \left(\frac{X_L \,||\, R_R \,||\, R_A}{X_L \,||\, R_R \,||\, R_A + R_7}\right) V_G$$

$$V_G = A\left[u(t) - u(t-a) + u(t-2a) - \cdots\right]$$

$$X_L \,||\, R_R \,||\, R_A = \frac{\left(\frac{R_R R_A}{R_R + R_A}\right) X_L}{\frac{R_R R_A}{R_R + R_A} + X_L}$$

$$\therefore V_{R_A} = \frac{\left(\frac{\frac{R_R X_L}{R_R + R_A}}{\frac{R_R R_A}{R_R + R_A} + X_L}\right) A\left[u(t) - u(t-a) + u(t-2a) - \cdots\right]}{\left(\frac{\frac{R_R R_A X_L}{R_R + R_A}}{\frac{R_R R_A}{R_R + R_A} + X_L}\right) + R_7}$$

B-2

where

I_{R_A} = current into R_A

V_{R_A} = voltage across R_A

R_A = effective impedance of the input to the amplifying portion of the detector

X_L = impedance of the a-c winding of the transformer, T_1

V_G = output voltage of square wave generator

A = amplitude of V_G

$u(t)$, $u(t-a)$ $\cdots$ = time displaced unit step functions

It is evident that as R_R decreases, V_{R_A} and I_{R_A} decrease, thus reducing the voltage (and hence the base current of Q_4) available to the amplifying portion of the detector.

In the form described here, the effective active region of each detector is a range of third-terminal potentials from approximately 125 to 250 mv; this input requires a maximum of 150 μa from the third terminal. The static input impedance of each detector is greater than 500 ohms. The dynamic input impedance of each detector at a third-terminal potential of 250 mv is 1.6 kilohms.

The initial point of the active region (sensitivity) of these detectors can be varied from zero up to several hundred volts by a proper choice of the detector diode, D_6, and Resistor R_8. Conventional diodes or stabistors are used for the low voltage range and Zeners can be used for high voltages.

The width of the active region is also affected slightly by the choice of D_6 and R_8, but in the main is set by the choice of R_4 and R_5 immediately following the detector outputs. The input impedance and current required from the third terminal will vary accordingly.

The full control circuit described in this report was designed for a five-cell pack. However, virtually any number of cells can be accommodated, since Transformer T_1 in each detector affords complete isolation between cells and between each cell and the circuitry which follows it. Also the node to which all detector outputs are connected constitutes an OR circuit which gives both control logic and electrical isolation between individual detector outputs.
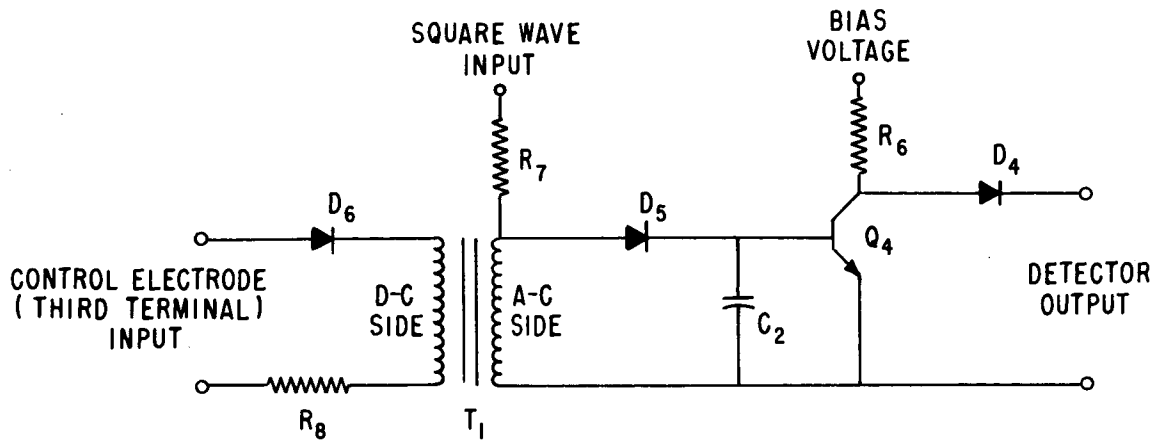
USN MARINE ENGINEERING LABORATORY
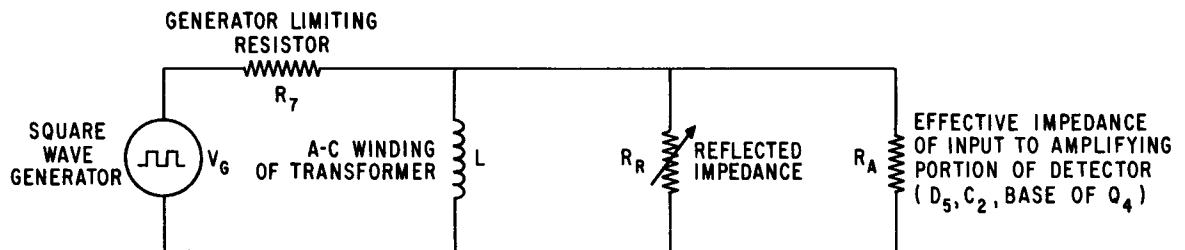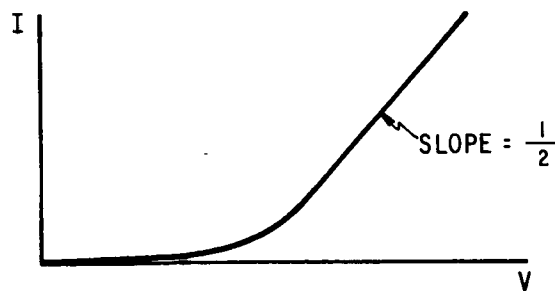
Figure 1-B - Detector

Figure 2-B - Equivalent Circuit of Diode Detector

Figure 3-B - Characteristic Curve of D_6, R_8 Combination

DOCUMENT CONTROL DATA - R&D

(Security classification of title, body of abstract and indexing annotation must be entered when the overall report is classified)

1. ORIGINATING ACTIVITY *(Corporate author)*	2a. REPORT SECURITY CLASSIFICATION
U. S. Navy Marine Engineering Laboratory Annapolis, Maryland 21402	Unclassified
	2b. GROUP

3. REPORT TITLE

Charge-Current Control Circuit for Nickel-Cadmium Cells with Control Electrodes

4. DESCRIPTIVE NOTES *(Type of report and inclusive dates)*

Final report

5. AUTHOR(S) *(Last name, first name, initial)*

Liwski, P. P. M.

6. REPORT DATE	7a. TOTAL NO. OF PAGES	7b. NO. OF REFS
April 1965	11	

8a. CONTRACT OR GRANT NO.	9a. ORIGINATOR'S REPORT NUMBER(S)
b. PROJECT NO.	25/65
c.	9b. OTHER REPORT NO(S) *(Any other numbers that may be assigned this report)*
d.	61 501

10. AVAILABILITY/LIMITATION NOTICES

Qualified requesters may obtain copies of this report from DDC.

11. SUPPLEMENTARY NOTES	12. SPONSORING MILITARY ACTIVITY
	National Aeronautics and Space Admin Greenbelt, Maryland

13. ABSTRACT

A circuit to control charge current entering nickel-cadmium cells with control electrodes ("three-terminal" cells) has been developed by MEL for use in systems requiring minimum space and weight with optimum control. The potential on the third (control) electrode of a cell becomes input to determine time and manner of charge-current change. Presently a laboratory instrument, this circuit is later to be adapted to satellite applications.

(Author)

DD _{1 JAN 64} **FORM** **1473**